β decay of even-A nuclei within the interacting boson model with input based on nuclear density functional theory

Nomura, Kosuke; Rodríguez-Guzmán, R.; Robledo, L. M.

β decay of even-A nuclei within the interacting boson model with input based on nuclear density functional theory

K. Nomura,[1,*] R. Rodríguez-Guzmán,[2] and L. M. Robledo[3,4]

[1]*Department of Physics, Faculty of Science, University of Zagreb, HR-10000 Zagreb, Croatia*
[2]*Physics Department, Kuwait University, 13060 Kuwait, Kuwait*
[3]*Departamento de Física Teórica, Universidad Autónoma de Madrid, E-28049 Madrid, Spain*
[4]*Center for Computational Simulation, Universidad Politńica de Madrid, Campus de Montegancedo, Bohadilla del Monte, E-28660-Madrid, Spain*

(Received 27 February 2020; accepted 14 April 2020; published 30 April 2020)

We compute the β-decay ft values within the frameworks of the energy density functional (EDF) and the interacting boson model (IBM). Based on the constrained mean-field calculation with the Gogny-D1M EDF, the IBM Hamiltonian for an even-even nucleus and essential ingredients of the interacting boson-fermion-fermion model (IBFFM) for describing the neighboring odd-odd nucleus are determined in a microscopic way. Only the boson-fermion and residual neutron-proton interaction strengths are determined empirically. The Gamow-Teller (GT) and Fermi (F) transition rates needed to compute the β-decay ft values are obtained without any additional parameter or quenching of the g_A factor. The observed log ft values for the β^+ decays of the even-even Ba into odd-odd Cs nuclei, and of the odd-odd Cs to the even-even Xe nuclei, with mass $A \approx 130$ are reasonably well described. The predicted GT and F transition rates represent a sensitive test of the quality of the IBM and IBFFM wave functions.

DOI: 10.1103/PhysRevC.101.044318

I. INTRODUCTION

The β decay of atomic nuclei is a consequence of electroweak fundamental processes and its ability to convert protons in neutrons and vice versa make it a very relevant reaction mechanism in many nuclear physics scenarios. For instance, β decay plays an important role in modeling the creation of elements in astrophysical nucleosynthesis scenarios. Precise measurement and the theoretical description of the (single) β decay are also crucial to better estimating the matrix element of the $\beta\beta$ decay, especially the one that does not emit neutrinos (neutrinoless $\beta\beta$ decay), a rare event that would signal the existence of physics beyond the standard model of elementary particles [1,2].

The quantitative understanding of the β-decay process requires a good and consistent description of the low-lying spectrum of both parent and daughter nuclei. A variety of theoretical methods have been used for this purpose. Without trying to be exhaustive, we can mention the quasiparticle random phase approximation (QRPA) used at various levels of sophistication [3–8], the beyond mean-field approaches within the nuclear energy density functional (EDF) framework [9,10], the description based on large-scale interacting shell model calculations [11–15], or that based on the interacting boson model (IBM) [16–25]. Each of the theoretical methods have their own advantages and drawbacks that defined their range of applicability in the nuclear chart.

In the present work, we employ the IBM framework with input from microscopic EDF calculations [26]. Our principal aim is a consistent theoretical description of the low-lying states and β decay of even-A nuclei, including even-even and odd-odd ones. Within this approach, the potential energy surface (PES) for a given even-even nucleus is computed microscopically by means of the constrained mean-field method based on a nuclear EDF. The mean-field PES is mapped onto the expectation value of the IBM Hamiltonian in the intrinsic state of the s (with spin and parity 0^+) and d (2^+) boson system. This procedure completely determines the strength parameters of the IBM Hamiltonian, which provides excitation spectra and transition strengths in arbitrary nuclear systems. The method can be extended to odd-mass and odd-odd nuclear systems by using the particle-boson coupling scheme. In such an extension, an additional EDF mean-field calculation is carried out to provide the required spherical single-particle energies and occupation numbers for unpaired nucleon(s) in the odd-A or odd-odd nucleus. Those mean-field quantities represent an essential input to build the Hamiltonian of the interacting boson-fermion-fermion model (IBFFM) [18,27]. The strength parameters for the boson-fermion and residual neutron-proton coupling terms are determined so as to reproduce reasonably well the experimental low-energy spectra in the neighboring odd-A nucleus, and the odd-odd nucleus of interest. At the price of having to determine these few coupling constants empirically, the method allows for a systematic, detailed and simultaneous description of spectroscopy in even-even, odd-A, and odd-odd nuclei in a computationally feasible manner as also required in β-decay studies.

*knomura@phy.hr

In Ref. [28], we implemented the EDF-based interacting boson-fermion model (IBFM) [18,29] approach in the study of the β decay of odd-A nuclei. There we studied the allowed β decays, where the spin of the parent nucleus changes according to the $\Delta I = 0, \pm 1$ rule and parity is conserved. Both the Gamow-Teller (GT) and Fermi (F) transition strengths were considered in the evaluation of the ft values of the β decay. One of the advantages of our approach is that the calculation for the GT and F transition rates does not involve any additional free parameter, and that can be considered a very stringent test for the IBFM wave functions for the parent and daughter nuclei.

In the present work, since we are focusing on β decay between even-mass nuclei, the calculation of the ft values requires the IBM and IBFFM wave functions for the parent and daughter (or vise versa) even-even and odd-odd nuclei, respectively. Calculation of the single-β decay between such even-A nuclei is also required for computing the $\beta\beta$ decay nuclear matrix elements, which are suggested to occur between a number of even-even nuclei. As in Ref. [28], we consider the β decays of those nuclei in the $A \approx 130$ mass region. There are a number of (phenomenological) IBFM calculations for the low-lying states and β decay of odd-A nuclei. However, application of the IBFFM framework to the spectroscopy in odd-odd nuclear systems has rarely been pursued, let alone their β decays. To the best of our knowledge, the IBFFM has been employed to study the β decays only in Refs. [22] and [24]. The former study is a first attempt to implement IBFFM in the β decay of even-even system, but only one nucleus ^{124}Ba was considered there. In the latter reference, two-neutrino $\beta\beta$ decays from Te to Xe isotopes was explored. The results of both studies are encouraging, since they show that the IBFFM framework is capable of describing the β decay of even-A nuclei, even though the IBFFM Hamiltonian was determined in a fully phenomenological way.

We have used the parametrization D1M [30] of the Gogny-EDF [31,32] for the microscopic calculation of the PES. Previous studies, using the EDF-to-IBM mapping procedure, have shown that the Gogny-D1M EDF provides a reasonable description of the spectroscopic properties of odd-A and odd-odd nuclei [33–36] in variety of mass regions including medium mass and heavy nuclei.

This paper is outlined as follows. In Sec. II we briefly describe the procedures to build the IBFFM Hamiltonians from the constrained Gogny-EDF calculations, and introduce the β-decay operators. The results of our calculations for the low-lying energy levels of the even-even Xe and Ba, and odd-odd Cs nuclei are briefly reviewed in Sec. III. The log ft values obtained for the β decays of the studied even-A nuclei are discussed in Sec. IV. Finally, Sec. V is devoted to the summary and the concluding remarks.

II. THEORETICAL FRAMEWORK

A. Hamiltonian

Let us first introduce the IBFFM Hamiltonian $\hat{H}$ for odd-odd systems. Note that we use the version of the IBFFM (called IBFFM-2) that distinguishes between neutron and proton degrees of freedom. The IBFFM-2 Hamiltonian consists of the IBM (called IBM-2) Hamiltonian $\hat{H}_{\rm B}$ for an even-even nucleus, the Hamiltonians $\hat{H}^{\rho}_{\rm F}$ for the odd neutron ($\rho = \nu$) and proton ($\rho = \pi$), the Hamiltonians $\hat{H}^{\rho}_{\rm BF}$ that couple the odd neutron and the odd proton to the IBM-2 core, and finally the residual neutron-proton interaction $\hat{V}_{\rm res}$:

$$\hat{H} = \hat{H}_{\rm B} + \hat{H}^{\nu}_{\rm F} + \hat{H}^{\pi}_{\rm F} + \hat{H}^{\nu}_{\rm BF} + H^{\pi}_{\rm BF} + \hat{V}_{\rm res}. \tag{1}$$

The IBM-2 Hamiltonian reads

$$\hat{H}_{\rm B} = \epsilon\left(\hat{n}_{d_\nu} + \hat{n}_{d_\pi}\right) + \kappa \hat{Q}_\nu \hat{Q}_\pi, \tag{2}$$

where $\hat{n}_{d_\rho} = d^\dagger_\rho \tilde{d}_\rho$ is the d-boson number operator, and $\hat{Q}_\rho = d^\dagger_\rho s_\rho + s^\dagger_\rho \tilde{d}^\dagger_\rho + \chi_\rho (d^\dagger_\rho \times \tilde{d}_\rho)^{(2)}$ is the quadrupole operator. The parameters of the Hamiltonian are denoted by ϵ, κ, χ_ν, and χ_π. The doubly magic nucleus ^{132}Sn is taken as the inert core for the boson space. The numbers of neutron N_ν and proton N_π bosons are computed as the numbers of neutron-hole and proton-particle pairs, respectively [37]. In the following, we will simplify the notation and we will refer to the IBM-2 and IBFFM-2 Hamiltonians simply as IBM and IBFFM, respectively.

The single-nucleon Hamiltonian $\hat{H}^{\rho}_{\rm F}$ is given as

$$\hat{H}^{\rho}_{\rm F} = -\sum_{j_\rho} \epsilon_{j_\rho} \sqrt{2j_\rho + 1} \left(a^\dagger_{j_\rho} \times \tilde{a}_{j_\rho}\right)^{(0)} \tag{3}$$

with ϵ_{j_ρ} being the single-particle energy of the odd nucleon. Here, j_ν (j_π) stands for the angular momentum of the single neutron (proton). The fermion creation and annihilation operators are denoted by $a^{(\dagger)}_{j_\rho}$ and $\tilde{a}_{j_\rho}$, with $\tilde{a}_{jm} = (-1)^{j-m} a_{j-m}$. For the fermion valence space, we consider the full neutron and proton major shell $N, Z = 50 - 82$, i.e., the $3s_{1/2}$, $2d_{3/2}$, $2d_{5/2}$, $1g_{7/2}$, and $1h_{11/2}$ orbitals.

The boson-fermion coupling Hamiltonian $\hat{H}^{\rho}_{\rm BF}$ takes the form

$$\hat{H}^{\rho}_{\rm BF} = \Gamma_\rho \hat{Q}_{\rho'} \hat{q}_\rho + \Lambda_\rho \hat{V}_{\rho'\rho} + A_\rho \hat{n}_{d_\rho} \hat{n}_\rho, \tag{4}$$

where $\rho' \neq \rho$. The first, second, and third terms in the expression above are the quadrupole dynamical, exchange, and monopole terms, respectively. The strength parameters are denoted by Γ_ρ, Λ_ρ, and A_ρ. As in previous studies [38,39] we assume that both the quadrupole dynamical and exchange terms are dominated by the interaction between unlike particles (i.e., between the odd neutron and proton bosons and between the odd proton and neutron bosons). On the other hand, for the monopole term we only consider the interaction between like-particles (i.e., between the odd neutron and neutron bosons and between the odd proton and proton bosons). The bosonic quadrupole operator $\hat{Q}_\rho$ in Eq. (4) is the same as the one used in Eq. (2). The fermionic quadrupole operator $\hat{q}_\rho$ reads

$$\hat{q}_\rho = \sum_{j_\rho j'_\rho} \gamma_{j_\rho j'_\rho} \left(a^\dagger_{j_\rho} \times \tilde{a}_{j'_\rho}\right)^{(2)}, \tag{5}$$

where $\gamma_{j_\rho j'_\rho} = (u_{j_\rho} u_{j'_\rho} - v_{j_\rho} v_{j'_\rho}) Q_{j_\rho j'_\rho}$ and $Q_{j_\rho j'_\rho} = \langle l \tfrac{1}{2} j_\rho || Y^{(2)} || l' \tfrac{1}{2} j'_\rho \rangle$ represents the matrix element of the fermionic quadrupole operator in the considered single-particle basis.

The exchange term $\hat{V}_{\rho'\rho}$ in Eq. (4) reads

$$\hat{V}_{\rho'\rho} = -(s^\dagger_{\rho'}\tilde{d}_{\rho'})^{(2)}\Bigg\{\sum_{j_\rho j'_\rho j''_\rho}\sqrt{\frac{10}{N_\rho(2j_\rho+1)}}\beta_{j_\rho j'_\rho}\beta_{j''_\rho j_\rho}\,:$$
$$\left(\left(d^\dagger_\rho\times\tilde{a}_{j''_\rho}\right)^{(j_\rho)}\times\left(a^\dagger_{j'_\rho}\times\tilde{s}_\rho\right)^{(j'_\rho)}\right)^{(2)}:\Bigg\}+(\text{H.c.}) \quad (6)$$

with $\beta_{j_\rho j'_\rho} = (u_{j_\rho}v_{j'_\rho} + v_{j_\rho}u_{j'_\rho})Q_{j_\rho j'_\rho}$. In the second line of the expression above the notation $:(\cdots):$ indicates normal ordering. The definition of the number operator for the odd fermion in the monopole interaction has already appeared in Eq. (3).

For the residual neutron-proton interaction $\hat{V}_{\rm res}$, we adopted the following form:

$$\hat{V}_{\rm res} = 4\pi u_{\rm D}\delta(\mathbf{r}) + u_{\rm T}\left\{\frac{3(\sigma_\nu\cdot\mathbf{r})(\sigma_\pi\cdot\mathbf{r})}{r^2} - \sigma_\nu\sigma_\pi\right\}, \quad (7)$$

where the first and second terms denote the δ and tensor interactions, respectively. We have found that these two terms are enough to provide a reasonable description of the low-lying states in the considered odd-odd nuclei. Note that by definition $\mathbf{r} = \mathbf{r}_\nu - \mathbf{r}_\pi$ and that $u_{\rm D}$ and $u_{\rm T}$ are the parameters of this term. Furthermore, the matrix element $V'_{\rm res}$ of the residual interaction $\hat{V}_{\rm res}$ can be expressed as [24]

$$V'_{\rm res} = \left(u_{j'_\nu}u_{j'_\pi}u_{j_\nu}u_{j_\nu} + v_{j'_\nu}v_{j'_\pi}v_{j_\nu}v_{j_\nu}\right)V^J_{j'_\nu j'_\pi j_\nu j_\pi}$$
$$-\left(u_{j'_\nu}v_{j'_\pi}u_{j_\nu}v_{j_\pi} + v_{j'_\nu}u_{j'_\pi}v_{j_\nu}u_{j_\pi}\right)$$
$$\times\sum_{J'}(2J'+1)\begin{Bmatrix} j'_\nu & j_\pi & J' \\ j_\nu & j'_\pi & J\end{Bmatrix}V^{J'}_{j'_\nu j_\pi j_\nu j'_\pi}, \quad (8)$$

where

$$V^J_{j'_\nu j'_\pi j_\nu j_\pi} = \langle j'_\nu j'_\pi; J|\hat{V}_{\rm res}|j_\nu j_\pi; J\rangle \quad (9)$$

represents the matrix element between the neutron-proton pair with angular momentum J. The bracket in Eq. (8) represents the corresponding Racah coefficient. As was done in Ref. [40], the terms resulting from contractions are neglected in Eq. (8).

The matrix form of the IBFFM Hamiltonian of Eq. (1) is obtained in the basis $|[L_\nu\otimes L_\pi]^{(L)}\otimes[j_\nu\otimes j_\pi]^{(J)}]^{(I)}\rangle$. Here, L_ρ is the angular momentum of proton or neutron boson system, L is the total angular momentum of the boson system, and I is the total angular momentum of the coupled boson-fermion-fermion system.

B. Procedure to build the IBFFM Hamiltonian

As the first step to build the IBFFM Hamiltonian, we have carried out (constrained) Hartree-Fock-Bogoliubov (HFB) calculations, based on the parametrization D1M of the Gogny-EDF. Those HFB calculations provide the potential energy surfaces (PESs), in terms of the quadrupole deformation parameters β and γ, for the even-even core nuclei $^{124-132}$Xe and $^{124-132}$Ba. For a given nucleus, the Gogny-D1M PES is then mapped onto the expectation value of the IBM-2 Hamiltonian in the boson coherent state [41] (see, Refs. [26,42] for details). This mapping procedure uniquely determines the parameters ϵ, κ, χ_ν, and χ_π in the boson Hamiltonian. Their values have already been given in Ref. [28].

Second, the single-particle energies ϵ_{j_ν} (ϵ_{j_π}) and occupation probabilities $v^2_{j_\nu}$ ($v^2_{j_\pi}$) of the unpaired neutron (proton) for the neighboring odd-N (odd-Z) nucleus are computed with the help of Gogny-D1M HFB calculations constrained to zero deformation [33]. Those energies are used as input to the Hamiltonians $\hat{H}^\nu_{\rm F}$ ($\hat{H}^\pi_{\rm F}$) and $\hat{H}^\nu_{\rm BF}$ ($\hat{H}^\pi_{\rm BF}$), for the odd-N Xe and odd-Z Cs isotopes, respectively. The optimal values of the strength parameters for the boson-fermion Hamiltonian $\hat{H}^\nu_{\rm BF}$ ($\hat{H}^\pi_{\rm BF}$), i.e., Γ_ν, Λ_ν, and A_ν (Γ_π, Λ_π, and A_π), are chosen separately for positive and negative parity, so as to reproduce the experimental low-energy spectrum for each of the considered odd-N Xe (odd-Z Cs) nuclei.

Third, the use the previous strength parameters Γ_ν, Λ_ν, and A_ν (Γ_π, Λ_π, and A_π) for the IBFFM Hamiltonian for the odd-odd nuclei $^{124-132}$Cs. In this case, the values of ϵ_{j_ρ} and $v^2_{j_\rho}$ are calculated again for each of these odd-odd nuclei. The employed boson-fermion interaction strengths, and ϵ_{j_ρ} and $v^2_{j_\rho}$ for the odd-odd Cs nuclei can be found in Ref. [36]. Finally, the strength parameters for the residual neutron-proton interaction, $u_{\rm D} = 0.7$ MeV and $u_{\rm T} = 0.02$ MeV, are taken also from Ref. [36].

C. Gamow-Teller and Fermi transition operators

To obtain the β-decay ft values, the Gamow-Teller (GT) and Fermi (F) matrix elements should be computed by using the IBM and IBFFM wave functions that correspond to the initial state (with spin $|I_{\rm i}\rangle$) for the parent nucleus and the final state (with spin $|I_{\rm f}\rangle$) for the daughter nucleus, or vice versa. The building blocks are the following one-fermion transfer operators [16]:

$$A^{(j)\dagger}_m = \zeta_j a^\dagger_{jm} + \sum_{j'}\zeta_{jj'}s^\dagger_\rho(\tilde{d}_\rho\times a^\dagger_{j'})^{(j)}_m, \quad (10)$$

$$B^{(j)\dagger}_m = \theta_j s^\dagger_\rho\tilde{a}_{jm} + \sum_{j'}\theta_{jj'}(d^\dagger_\rho\times\tilde{a}_{j'})^{(j)}_m. \quad (11)$$

Both operators increase the number of valence neutrons (protons) $n_j + 2N_\rho$ by one. Note, that the index of j_ρ is omitted for the sake of simplicity. The conjugate operators read

$$\tilde{A}^{(j)}_m = \zeta^*_j\tilde{a}_{jm} + \sum_{j'}\zeta^*_{jj'}s_\rho(d^\dagger_\rho\times\tilde{a}_{j'})^{(j)}_m, \quad (12)$$

$$\tilde{B}^{(j)}_m = -\theta^*_j s_\rho a^\dagger_{jm} - \sum_{j'}\theta^*_{jj'}(\tilde{d}_\rho\times a^\dagger_{j'})^{(j)}_m. \quad (13)$$

These operators decrease the number of valence neutrons (protons) $n_j + 2N_\rho$ by one.

The coefficients ζ_j, $\zeta_{jj'}$, θ_j, and $\theta_{jj'}$ in Eqs. (10)–(13) are given [18] by

$$\zeta_j = u_j\frac{1}{K'_j}, \quad (14)$$

$$\zeta_{jj'} = -v_j\beta_{j'j}\sqrt{\frac{10}{N_\rho(2j+1)}}\frac{1}{KK'_j}, \quad (15)$$

$$\theta_j = \frac{v_j}{\sqrt{N_\rho}}\frac{1}{K''_j}, \tag{16}$$

$$\theta_{jj'} = u_j\beta_{j'j}\sqrt{\frac{10}{2j+1}}\frac{1}{KK''_j}. \tag{17}$$

The parameters K, K'_j, and K''_j entering the previous expressions read [16,18,43]

$$K = \left(\sum_{jj'}\beta^2_{jj'}\right)^{1/2}, \tag{18a}$$

$$K'_j = \left(1 + 2\left(\frac{v_j}{u_j}\right)^2\frac{\langle(\hat{n}_{s_\rho}+1)\hat{n}_{d_\rho}\rangle_{0^+_1}}{N_\rho(2j+1)}\frac{\sum_{j'}\beta^2_{j'j}}{K^2}\right)^{1/2}, \tag{18b}$$

$$K''_j = \left(\frac{\langle\hat{n}_{s_\rho}\rangle_{0^+_1}}{N_\rho} + 2\left(\frac{u_j}{v_j}\right)^2\frac{\langle\hat{n}_{d_\rho}\rangle_{0^+_1}}{2j+1}\frac{\sum_{j'}\beta^2_{j'j}}{K^2}\right)^{1/2}. \tag{18c}$$

In these definition, $\hat{n}_{s_\rho}$ is the number operator for the s_ρ boson and $\langle\cdots\rangle_{0^+_1}$ represents the expectation value of a given operator in the 0^+_1 ground state of the considered even-even nucleus. For a more detailed account, the reader is referred to Refs. [16,18,43].

The boson images of the Fermi ($t^\pm$) and Gamow-Teller ($t^\pm\sigma$) transition operators, denoted by $\hat{O}^{\rm F}$ and $\hat{O}^{\rm GT}$, respectively, take the form

$$t^\pm \longmapsto \hat{O}^{\rm F} = -\sum_j \sqrt{2j+1}\left(P^{(j)}_\nu \times P^{(j)}_\pi\right)^{(0)}, \tag{19}$$

$$t^\pm\sigma \longmapsto \hat{O}^{\rm GT} = \sum_{j'j}\eta_{j'j}\left(P^{(j')}_\nu \times P^{(j)}_\pi\right)^{(1)}, \tag{20}$$

where the $\eta_{j'j}$ coefficients are proportional to the reduced matrix elements of the spin operator

$$\eta_{j'j} = -\frac{1}{\sqrt{3}}\left\langle \ell'\frac{1}{2}; j'||\sigma||\ell\frac{1}{2}; j\right\rangle = -\delta_{\ell'\ell}\sqrt{2(2j'+1)(2j+1)}W\left(\ell j'\frac{1}{2}1;\frac{1}{2}j\right) \tag{21}$$

with W being a Racah coefficient. In the case of β^+ decay $P^{(j')}_\nu = \tilde{B}^{(j')}_\nu$ and $P^{(j)}_\pi = \tilde{A}^{(j)}_\pi$ while for β^- decay $P^{(j')}_\nu = B^{(j')\dagger}_\nu$ and $P^{(j)}_\pi = A^{(j)\dagger}_\pi$. Then, the reduced Fermi $\langle M_{\rm F}\rangle$ and Gamow-Teller $\langle M_{\rm GT}\rangle$ matrix elements read

$$\langle M_{\rm F}\rangle = \frac{1}{\sqrt{2I_{\rm i}+1}}|\langle I_{\rm f}||\hat{O}^{\rm F}||I_{\rm i}\rangle|, \tag{22}$$

$$\langle M_{\rm GT}\rangle = \frac{1}{\sqrt{2I_{\rm i}+1}}|\langle I_{\rm f}||\hat{O}^{\rm GT}||I_{\rm i}\rangle|. \tag{23}$$

The ft value for the β decay $I_{\rm i} \to I_{\rm f}$, can be computed, in seconds, using the expression

$$ft = \frac{6163}{\langle M_{\rm F}\rangle^2 + g_A^2\langle M_{\rm GT}\rangle^2}. \tag{24}$$

The quantity g_A is the ratio of the axial-vector to vector coupling constants, $g_A = G_A/G_V$. We have employed the free nucleon value $g_A = 1.2701(25)$ [44] for all the studied nuclei without quenching.

III. LOW-ENERGY STRUCTURE OF THE PARENT AND DAUGHTER NUCLEI

The low-lying level structure and electromagnetic properties of the even-even Ba and Xe, as well as odd-odd Cs, nuclei have already been discussed in detail in Ref. [36]. Also in this reference, the IBFM description of the neighboring odd-N Ba and Xe as well as odd-Z Cs isotopes has been amply discussed and shown to be also in reasonable agreement with experiment. The even-even $^{124-132}$Xe nuclei are taken as the cores for the odd-odd $^{124-132}$Cs nuclei. The Gogny-HFB PESs and mapped IBM description of these even-even Xe nuclei have shown that quite many of them are γ-soft [34]. Therefore, the low-energy spectra of the odd-odd Cs nuclei are described in terms of an unpaired neutron hole and a proton coupled to the γ-soft even-even core Xe nuclei. The low-energy positive-parity states of the odd-odd Cs nuclei, with excitation energies typically up to $E_{\rm exc} \approx 0.4$ MeV, have been shown [36] to be built on the $(\nu sdg)^{-1} \otimes (\pi sdg)^1$ neutron-proton pair configuration.

The low-energy spectra for the even-even $^{124-132}$Ba and $^{124-132}$Xe isotopes are shown in Fig. 1. The IBM description of the low-lying excited states of the even-even systems looks very nice. An exception is perhaps the excitation energy of the 0^+_2 level in many of the Ba nuclei, which is overestimated by the calculation. This is because the Gogny-HFB PESs have a minimum at a rather large deformation leading to a rather pronounced rotational energy spectrum in the IBM calculation. Also in Fig. 1, the calculated and experimental positive-parity excitation spectra for the odd-odd $^{124-132}$Cs nuclei are depicted up to 0.4 MeV excitation energy. Note that the energy spectra for the odd-odd Cs, shown in the figure, are taken from Ref. [36] without any modification. Except for the ^{132}Cs nucleus, the IBFFM reproduces the correct ground-state spin. The calculation is not able to describe all the details of the lowest-lying level structures in each nucleus. But this is not surprising, considering the presence of both the unpaired neutron and proton degrees of freedom.

There are also those higher-spin positive-parity states with an excitation energy of $E_{\rm exc} \geqslant 0.4$ MeV and with a spin typically $I \geqslant 6^+$. These high-spin states are mostly accounted for by the $(\nu h_{11/2})^{-1} \otimes (\pi h_{11/2})^1$ configuration, and are considered to be members of a chiral band. Note, however, that most of the β decays considered in this work are relevant only for the low-spin states, i.e., $I \leqslant 4^+$, of the odd-odd Cs. Furthermore, the admixture of the $(\nu h_{11/2})^{-1} \otimes (\pi h_{11/2})^1$ pair configuration into the lowest-lying states is so small, that its effect on the β-decay rates from and to the ground states of the odd-odd Cs can be considered as negligible.

Other spectroscopic properties of the low-lying states of the even-even Xe and Ba and odd-odd Cs isotopes, such as the electric quadrupole and magnetic dipole moments and transition strengths, were described reasonably well [36].

IV. β DECAY

A. β decays of even-even Ba

We show in Fig. 2 the predicted $\log ft$ values for the β^+ decay [electron-capture (EC)] of the even-A nuclei,

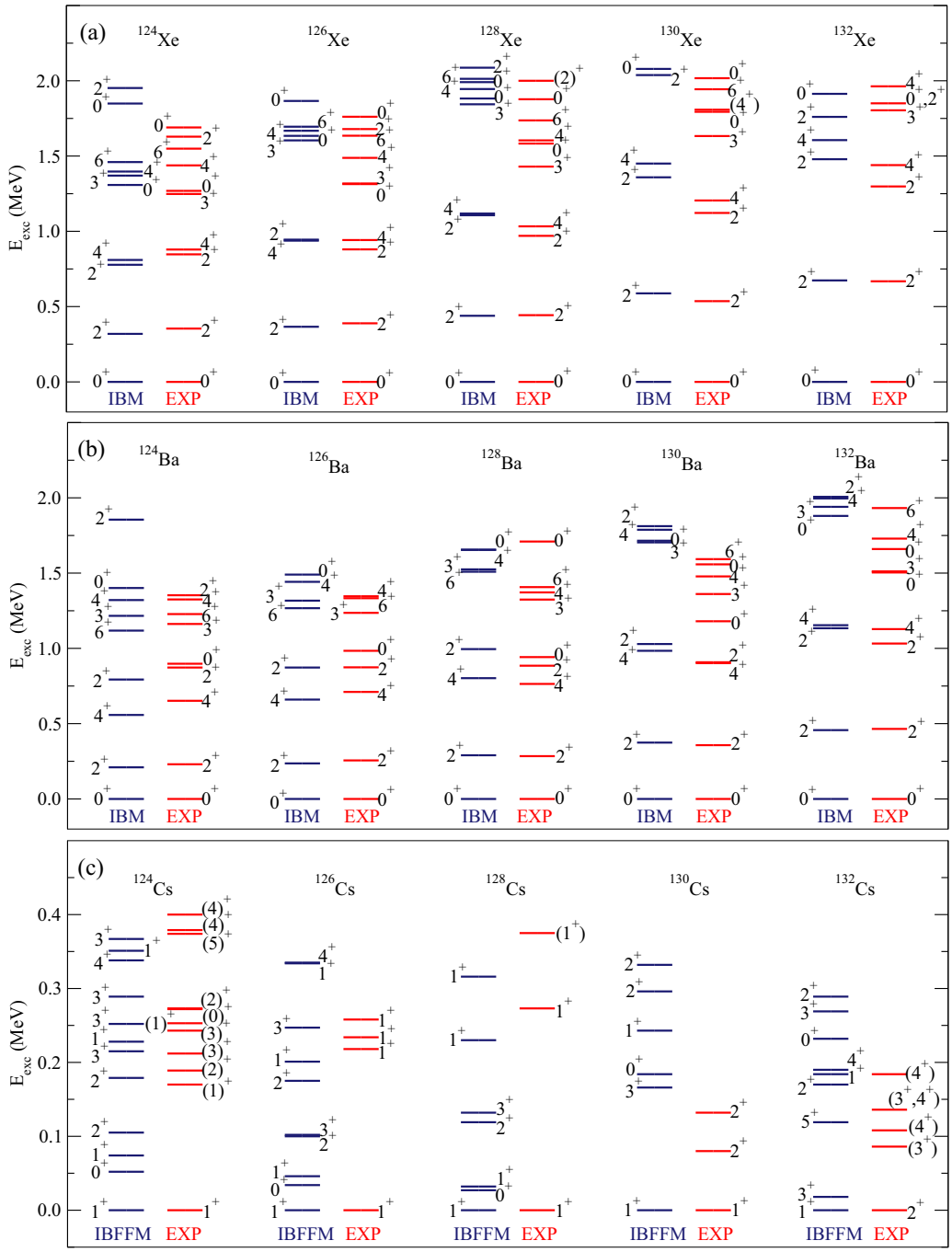

FIG. 1. Low-energy and low-spin excitation spectra for the even-even $^{124-132}$Xe and $^{124-132}$Ba, and the odd-odd $^{124-132}$Cs nuclei considered in this work. The experimental data are taken from the compilation of the ENSDF database [45].

that is, $^{124-132}\mathrm{Ba}(0_1^+) \rightarrow {}^{124-132}\mathrm{Cs}(1_1^+)$, and $^{124-132}\mathrm{Cs}(1_1^+) \rightarrow {}^{124-132}\mathrm{Xe}(0_1^+)$ [panel (a)], and $^{124-132}\mathrm{Ba}(0_1^+) \rightarrow {}^{124-132}\mathrm{Cs}(0_1^+)$, and $^{124-130}\mathrm{Cs}(0_1^+) \rightarrow {}^{124-130}\mathrm{Xe}(0_1^+)$ [panel (b)]. The experimental data are taken from the ENSDF database [45] and are also depicted in the figure. The calculated $\log ft$ values for the ground-state–to–ground-state decays 0_1^+(Ba)$\rightarrow 1_1^+$(Cs) are in a very good agreement with the experiment. The $\log ft$ values for the 1_1^+(Cs)$\rightarrow 0_1^+$(Xe) decays are, however, considerably overestimated. The $0_1^+ \leftrightarrows 1_1^+$ decays involve only the GT transitions, and the $\langle M_{\mathrm{GT}}\rangle^2$ values for these decays appear to be too small in our calculation. We will discuss below the reason for this small matrix elements. As for the $0_1^+ \rightarrow 0_1^+$ decays [see Fig. 2(b)], where only the Fermi transition enters, the present calculation gives a very good description of the experimental $\log ft$ values for the decays of ^{124,126}Ba into ^{124,126}Cs nuclei. A characteristic systematic trend of the predicted $\log ft$ value is that for both the $\Delta I = \pm 1$ [Fig. 2(a)] and $\Delta I = 0$ [Fig. 2(b)] decays it changes abruptly between $N = 72$ and $N = 76$ (for the Ba $\rightarrow$ Cs decays) and between $N = 73$ and $N = 77$ (for

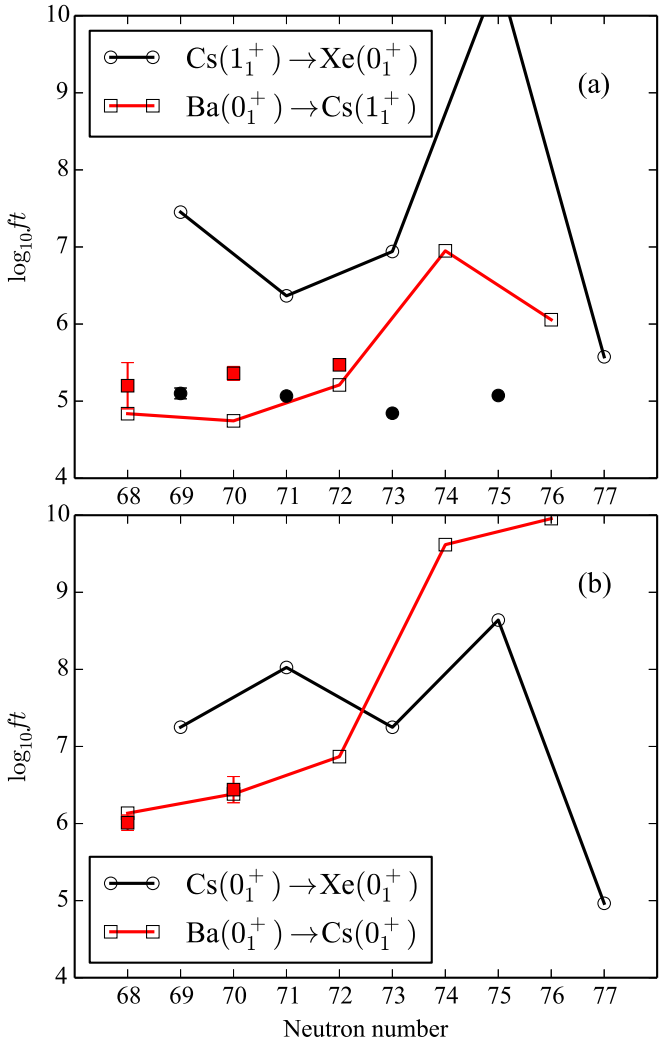

FIG. 2. The predicted log ft values (open symbols connected by solid lines) for the β^+ decays/EC (electron capture) between even-A nuclei, i.e., (a) Ba(0_1^+) → Cs(1_1^+), and Cs(1_1^+) → Xe(0_1^+), and (b) Ba(0_1^+) → Cs(0_1^+), and Cs(0_1^+) → Xe(0_1^+), plotted against the neutron number. The experimental log ft values, taken from the ENSDF database [45], are represented by filled circles (Cs → Xe decays) and squares (Ba → Cs decays).

TABLE I. The predicted and experimental log ft values in seconds for the β^+ decays/EC of the even-even ^{124,126,128}Ba into odd-odd ^{124,126,128}Cs nuclei. The experimental data have been taken from Ref. [45].

		log ft	
Decay	$I_i \to I_f$	Theory	Experiment
^{124}Ba → ^{124}Cs	$0_1^+ \to 0_1^+$	6.13	6.01(10)[a]
	$0_1^+ \to 1_1^+$	4.84	5.2(3)
	$0_1^+ \to 1_2^+$	5.90	5.07(7)
	$0_1^+ \to 1_3^+$	5.29	5.72(9)
	$0_1^+ \to 1_4^+$	6.30	6.01(10)[a]
	$0_1^+ \to 1_5^+$	4.60	6.04(9)[b]
	$0_1^+ \to 1_6^+$	4.95	6.23(10)[c]
	$0_1^+ \to 1_7^+$	5.18	6.83(16)[d]
	$0_1^+ \to 1_8^+$	5.44	4.54(7)[e]
^{126}Ba → ^{126}Cs	$0_1^+ \to 0_1^+$	6.35	6.44(17)
	$0_1^+ \to 1_1^+$	4.74	5.36(9)
	$0_1^+ \to 1_2^+$	4.82	6.36(12)
	$0_1^+ \to 1_3^+$	5.39	5.49(5)
	$0_1^+ \to 1_4^+$	5.62	6.44(17)
	$0_1^+ \to 1_5^+$	4.54	5.18(6)
	$0_1^+ \to 1_6^+$	6.03	5.12(7)
	$0_1^+ \to 1_7^+$	8.94	5.08(8)
	$0_1^+ \to 1_8^+$	10.81	4.54(7)
^{128}Ba → ^{128}Cs	$0_1^+ \to 0_1^+$	6.87	
	$0_1^+ \to 1_1^+$	5.20	5.471(9)
	$0_1^+ \to 1_2^+$	4.86	8.26(11)[f]
	$0_1^+ \to 1_3^+$	5.32	7.83(5)[g]
	$0_1^+ \to 1_4^+$	7.82	5.57(4)
	$0_1^+ \to 1_5^+$	4.78	7.83(9)[h]
	$0_1^+ \to 1_6^+$	6.78	7.33(7)[i]
	$0_1^+ \to 1_7^+$	8.60	6.68(6)

[a] $I = (0, 1)^+$ level at 272 keV in ^{124}Cs.
[b] $I = (1, 2)^+$ level at 401 keV in ^{124}Cs.
[c] $I = (1^+, 2^+)$ level at 404 keV in ^{124}Cs.
[d] $I = (1, 2)^+$ level at 444 keV in ^{124}Cs.
[e] $I = (1, 2)^+$ level at 557 keV in ^{124}Cs.
[f] $I = 0^-$, 1 level at 215 keV in ^{128}Cs.
[g] $I = 0^-$, 1 level at 230 keV in ^{128}Cs.
[h] $I = 0^-$, 1 level at 317 keV in ^{128}Cs.
[i] $I = 0^-$, 1 level at 359 keV in ^{128}Cs.

the Cs → Xe decays). Such an abrupt change in the log ft values could reflect the evolution of nuclear structure between axially symmetric and γ-soft deformed states. Accordingly, the structures of those wave functions for the boson-core Xe nuclei, as well as the neighboring odd-A Xe and Cs nuclei, are supposed to be very different between before and after the shape transition.

In Table I, we make a more detailed comparison between the predicted and experimental log ft values for the β^+ decays of the 0_1^+ ground states of even-even ^{124,126,128}Ba into those higher-lying states in odd-odd ^{124,126,128}Cs nuclei. Experimentally, there are many degenerate levels in those nuclei, and their spin and/or parities are also not firmly established. This makes very difficult to establish a one-to-one correspondence between the calculated and experimental log ft values. Those situations involving experimental degenerate levels are mentioned in the footnotes of Table I. The same rule applies to Tables II, III, and IV, in the following Sec. IV B. Among other things, we emphasize that, as seen from Table I, a very good agreement between the predicted and experimental log ft values is obtained for the β^+ decays to the 1_1^+ ground states of the ^{124,126,128}Cs nuclei. This situation is already shown in Fig. 2(a). In addition, the observed log ft values for the $0_1^+ \to 0_1^+$ decays of ^{124,126}Ba, where the GT transition is forbidden and only the Fermi transition enters, are well reproduced by our calculation. As for the log ft values for the decays into higher-energy, nonyrast 0^+ and 1^+ states, especially those higher than the fourth lowest-energy ones for each spin, the discrepancy between the calculation and experiment increases. We can understand this trend by taking

TABLE II. Same as Table I, but for the β^+/EC decays of the odd-odd ^{124}Cs to even-even ^{124}Xe nuclei.

		log ft	
Decay	$I_i \to I_f$	Theory	Experiment
^{124}Cs $\to$ ^{124}Xe	$1_1^+ \to 0_1^+$	7.45	5.10(7)
	$1_1^+ \to 0_2^+$	6.66	5.54(7)
	$1_1^+ \to 0_3^+$	6.62	6.21(7)
	$1_1^+ \to 0_4^+$	7.56	5.72(7)
	$1_1^+ \to 0_5^+$	7.50	5.69(7)[a]
	$1_1^+ \to 0_6^+$	10.27	6.6(4)[b]
	$1_1^+ \to 1_1^+$	5.81	6.6(4)[b]
	$1_1^+ \to 1_2^+$	6.02	5.69(7)[a]
	$1_1^+ \to 2_1^+$	6.06	5.10(7)
	$1_1^+ \to 2_2^+$	8.95	5.89(7)
	$1_1^+ \to 2_3^+$	8.63	5.73(7)
	$1_1^+ \to 2_4^+$	7.02	6.15(7)
	$1_1^+ \to 2_5^+$	7.25	6.01(7)
	$1_1^+ \to 2_6^+$	6.64	6.43(7)[c]
	$1_1^+ \to 2_7^+$	6.76	5.40(7)
	$1_1^+ \to 2_8^+$	6.71	5.69(7)[a]
	$7_1^+ \to 6_1^+$	6.97	7.4
	$7_1^+ \to 6_2^+$	7.80	7.7
	$7_1^+ \to 6_3^+$	10.60	7.6
	$7_1^+ \to 6_4^+$	8.34	6.2
	$7_1^+ \to 6_5^+$	8.86	7.3[d]
	$7_1^+ \to 7_1^+$	7.76	7.6
	$7_1^+ \to 7_2^+$	8.09	7.3[d]
	$7_1^+ \to 7_3^+$	8.69	6.7[e]
	$7_1^+ \to 7_4^+$	9.71	6.7[f]
	$7_1^+ \to 8_1^+$	7.65	7.3[d]
	$7_1^+ \to 8_2^+$	9.51	6.7[e]
	$7_1^+ \to 8_3^+$	8.63	6.7[f]

[a] $I = 0^+, 1^+, 2^+$ at 2536 keV in ^{124}Xe.
[b] $I = (0^+, 1, 2)$ at 3897 keV in ^{124}Xe.
[c] $I = 1^{(+)}, 2^{(+)}$ level at 2382 keV in ^{124}Xe
[d] $I = (6, 7, 8)^+$ level at 2979 keV in ^{124}Xe.
[e] $I = (6, 7, 8)^+$ level at 3739 keV in ^{124}Xe.
[f] $I = (6, 7, 8)^+$ level at 4093 keV in ^{124}Xe.

into account that the IBFFM is built in a reduced valence space, and the strength parameters are determined so as to fit the low-lying energy levels of odd-odd nuclei. Therefore, the wave functions for these higher non-yrast states in the present IBFFM calculation are not supposed to be as reliable as the ones of the lowest-energy states.

B. β decays of odd-odd Cs

Experimental data are more abundant for the β^+ decay of the odd-odd Cs isotopes. In Table II, the predicted log ft values for the decays of the 1_1^+ ground state of the ^{124}Cs nucleus into ^{124}Xe are compared with the experimental data. The log ft value for the decay to the $I_f = 0_1^+$ ground state of ^{124}Xe is predicted to be unexpectedly larger than the experimental one. This means that the calculated GT transition rate is too small. The dominant pair configurations in the IBFFM wave function for the 1_1^+ ground state are $[(\nu s_{1/2})^{-1} \otimes (\pi s_{1/2})^1]^{(J=1^+)}$ (14.2 %), $[(\nu s_{1/2})^{-1} \otimes (\pi d_{3/2})^1]^{(J=1^+)}$ (10.8 %), $[(\nu s_{1/2})^{-1} \otimes (\pi d_{5/2})^1]^{(J=3^+)}$ (12.8 %), and $[(\nu s_{1/2})^{-1} \otimes (\pi g_{7/2})^1]^{(J=3^+)}$ (11.2 %). The rest of the wave function is made up of numerous other components that are so small in their magnitudes as to be neglected. The odd neutron occupying the $3s_{1/2}$ orbital makes dominant contributions to the above mentioned pair configurations. This seems to be consistent with the fact that the $1/2_1^+$ ground state of the neighboring odd-A nucleus ^{123}Xe is mostly accounted for by the $3s_{1/2}$ neutron hole coupled to the even-even core ^{124}Xe [28].

TABLE III. Same as Table I, but for the β^+/EC decays of the odd-odd ^{126}Cs to even-even ^{126}Xe nuclei.

		log ft	
Decay	$I_i \to I_f$	Theory	Experiment
^{126}Cs $\to$ ^{126}Xe	$1_1^+ \to 0_1^+$	6.37	5.066(19)
	$1_1^+ \to 0_2^+$	6.83	5.39(3)
	$1_1^+ \to 0_3^+$	7.35	
	$1_1^+ \to 0_4^+$	7.08	6.93[a]
	$1_1^+ \to 0_5^+$	9.78	6.176(25)[b]
	$1_1^+ \to 0_6^+$	7.91	5.941(25)[c]
	$1_1^+ \to 0_7^+$	6.31	6.67(4)[d]
	$1_1^+ \to 0_8^+$	6.47	
	$1_1^+ \to 0_9^+$	9.45	6.09(3)[e]
	$1_1^+ \to 1_1^+$	6.16	>7.1[f]
	$1_1^+ \to 1_2^+$	7.64	6.93[a]
	$1_1^+ \to 1_3^+$	8.28	6.176(25)[b]
	$1_1^+ \to 2_1^+$	8.41	6.791(24)
	$1_1^+ \to 2_2^+$	4.43	7.574(20)
	$1_1^+ \to 2_3^+$	5.13	8.83(10)
	$1_1^+ \to 2_4^+$	5.56	6.306(12)
	$1_1^+ \to 2_5^+$	5.42	6.988(18)
	$1_1^+ \to 2_6^+$	7.35	>7.1[f]

[a] $I = 0^+, 1, 2$ level at 2229 keV in ^{126}Xe.
[b] $I = 0^+, 1, 2$ level at 2347 keV in ^{126}Xe.
[c] $I = 0^+, 1, 2$ level at 2503 keV in ^{126}Xe.
[d] $I = 0^+, 1, 2$ level at 2521 keV in ^{126}Xe.
[e] $I = 0^+, 1, 2$ level at 2796 keV in ^{126}Xe.
[f] $I = (1, 2^+)$ level at 2215 keV in ^{126}Xe.

Major contributions to the $\langle M_{\rm GT}\rangle$ value for the $1_1^+ \to 0_1^+$ decay of ^{124}Cs turn out to be from those terms proportional to $[a_{j_\nu}^\dagger \times a_{j_\pi}^\dagger]^{(1)}$, $[\tilde{d}_\nu \times [a_{j_\nu}^\dagger \times a_{j_\pi}^\dagger]]^{(1)}$, and $[\tilde{d}_\nu \times \tilde{d}_\pi] \times [a_{j_\nu}^\dagger \times a_{j_\pi}^\dagger]]^{(1)}$. Their matrix elements are calculated as 0.02886, -0.02576, and -0.02152, respectively. Two of these matrix elements have almost the equal magnitude but with opposite sign, and this leads to the too small $\langle M_{\rm GT}\rangle$ value. A similar kind of cancellation, among different components in $\langle M_{\rm GT}\rangle$ seems to take place in the GT transitions to the non-yrast 0^+ states of the daughter nucleus. In the previous IBFFM calculation for the β decay of ^{124}Ba in Ref. [22], the same kind of discrepancy (too large log ft values) was also found. The authors of Ref. [22] also attributed it to the cancellations of small components in the GT matrix element. On the other hand, for the decays with $\Delta I = 0$, i.e., $1_1^+ \to 1_1^+$, the predicted log ft values are generally smaller and reproduce

TABLE IV. Same as Table I, but for the β^+/EC decays of the odd-odd ^{128,130,132}Cs to even-even ^{128,130,132}Xe nuclei.

Decay	$I_i \to I_f$	log ft Theory	log ft Experiment
^{128}Cs → ^{128}Xe	$1_1^+ \to 0_1^+$	6.94	4.843(10)
	$1_1^+ \to 0_2^+$	7.24	5.579(24)
	$1_1^+ \to 0_3^+$	8.78	7.48(4)
	$1_1^+ \to 0_4^+$	6.74	5.70(3)
	$1_1^+ \to 1_1^+$	5.85	6.37(3)[a]
	$1_1^+ \to 1_2^+$	8.43	6.32(3)[b]
	$1_1^+ \to 1_3^+$	7.58	6.49(3)[c]
	$1_1^+ \to 2_1^+$	6.92	5.089(24)
	$1_1^+ \to 2_2^+$	7.39	5.829(25)
	$1_1^+ \to 2_3^+$	6.64	6.10(3)
	$1_1^+ \to 2_4^+$	6.77	6.37(3)[a]
	$1_1^+ \to 2_5^+$	7.13	6.24(3)
	$1_1^+ \to 2_6^+$	6.87	6.32(3)[b]
	$1_1^+ \to 2_7^+$	7.05	6.49(3)[c]
^{130}Cs → ^{130}Xe	$1_1^+ \to 0_1^+$	10.52	5.073(6)
	$1_1^+ \to 0_2^+$	6.33	7.0(1)
	$1_1^+ \to 0_3^+$	6.71	6.2(1)
	$1_1^+ \to 1_1^+$	6.80	6.9(2)[d]
	$1_1^+ \to 1_2^+$	8.37	
	$1_1^+ \to 2_1^+$	7.31	6.3(1)
	$1_1^+ \to 2_2^+$	5.23	7.5(4)
	$1_1^+ \to 2_3^+$	4.83	6.2(1)
	$1_1^+ \to 2_4^+$	7.56	6.9(2)[d]
^{132}Cs → ^{132}Xe	$1_1^+ \to 0_1^+$	5.58	
	$1_1^+ \to 0_2^+$	6.99	
	$1_1^+ \to 2_1^+$	6.38	
	$1_1^+ \to 2_2^+$	4.39	
	$2_1^+ \to 2_1^+$	6.36	6.679
	$2_1^+ \to 2_2^+$	4.46	8.7(1)
	$2_1^+ \to 2_3^+$	4.69	6.61(2)
	$2_1^+ \to 3_1^+$	6.37	7.17(2)

[a] $I = 1^+, 2^+, 3^+$ level at 2127 keV in ^{128}Xe.
[b] $I = (1, 2^+)$ level at 2362 keV in ^{128}Xe.
[c] $I = (1, 2^+)$ level at 2431 keV in ^{128}Xe.
[d] $I = 1, 2$ level at 2503 keV in ^{130}Xe.

the experimental data better than for the $\Delta I = \pm 1$ decays. This is mainly because $\langle M_F \rangle$ matrix elements also appear in the denominator in the expression for the ft-value for the $1_1^+ \to 1_1^+$ decays [see Eq. (24)].

In the case of the ^{124}Cs nucleus in particular, there are also the experimental data for the decays from the higher-spin state with $I_i = 7^+$. In the present IBFFM calculation, those states with spin higher than $I \approx 7^+$ are formed mainly of the $(\nu h_{11/2})^{-1} \otimes (\pi h_{11/2})^1$ neutron-proton pair configuration. In contrast, the low-spin and low-energy states in the vicinity of the ground state and with $I \leqslant 4^+$ are mainly based on the neutron and proton positive-parity sdg orbitals. The experimental log ft values for the decays of 7^+ state are generally log $ft \approx 7$, being larger than for the decays of the ground state 1_1^+, which are typically log $ft \approx$ 5–6. The description of the log ft values for this type of the β decay in the present calculation appears to be good, at least for the decays to the few lowest levels in the daughter nucleus. We confirmed that, as expected, the configurations that involve the neutron and proton unique-parity $h_{11/2}$ single-particle orbitals make significant contributions to the $\langle M_{GT} \rangle$ matrix elements for the decays of the $I_i = 7^+$ state.

The calculated log ft for the rest of the odd-odd Cs nuclei are shown in Tables III and IV and compared to the experimental data. Similarly to the ^{124}Cs → ^{124}Xe decay, the calculated log ft values for the decays of $^{126–132}$Cs, especially for the $\Delta I = \pm 1$ decays, are too large as compared with the experimental values. This appears to happen mainly because the cancellation between components of the $\langle M_{GT} \rangle$ matrix elements occurs to the extent that too small GT rates are obtained. On the other hand, the agreement with experimental data is relatively good for the $\Delta I = 0$ decays. Note, that a extremely large deviation is found in the decay ^{130}Cs$(1_1^+) \to {}^{130}$Xe(0_1^+) (see Table IV and also Fig. 2). The predicted ft value for this decay is larger than the experimental one implying a difference in the half-life of 5 orders of magnitude. Regarding the decay of the ^{132}Cs nucleus, where experimentally the 2_1^+ state is suggested to be the ground state, the present calculation reproduces very nicely the log ft value for the $2_1^+ \to 2_1^+$ decay.

V. SUMMARY AND CONCLUDING REMARKS

To summarize, the β decays of even-A nuclei are investigated within the EDF-based IBM approach. The even-even boson-core Hamiltonian, and essential building blocks of the particle-boson coupling Hamiltonians, i.e., single-particle energies and occupation probabilities of odd particles, are determined based on a fully microscopic mean field calculation with the Gogny EDF. A few coupling constants for the boson-fermion Hamiltonians, and for the residual neutron-proton interaction, remain as the only free parameters of the model. They are determined as to reasonably reproduce the low-energy levels of each of the neighboring odd-A and odd-odd nuclei. The IBM and IBFFM wave functions obtained after diagonalization of the corresponding Hamiltonians for the parent and daughter nuclei are used to calculate Gamow-Teller and Fermi matrix elements, which are required to compute the β-decay ft values. No additional parameter is introduced for the computations of the ft values. The g_A factor for the GT transition is not quenched in the present calculation.

The present work, as well as the preceding ones of Refs. [28,36], show that the employed theoretical method provides an excellent descriptions of the low-lying levels and electromagnetic transition rates in the relevant even-even Ba and Xe and odd-odd Cs, we as well as the neighboring odd-A Ba, Xe, and Cs nuclei. The observed β^+ decays/electron captures of the ground state 0_1^+ of the even-even ^{124,126,128}Ba into the 1_1^+ ground states and 0_1^+ states of ^{124,126,128}Cs are described very nicely. On the other hand, the log ft values for the $1^+ \to 0^+$ decays of the odd-odd Cs into even-even Xe nuclei are, in general, predicted to be too large with respect to the experimental values. It is shown that the deviation occurs mainly because numerous small components in the GT matrix element $\langle M_{GT} \rangle$ cancel each other, leading to the too small GT transition rates.

This is attributed to the combination of various factors in the adopted theoretical procedure, such as, the chosen boson-fermion coupling constants, residual neutron-proton interaction, and underlying microscopic inputs from the Gogny EDF.

The EDF-based IBM framework, employed here and in Ref. [28], represents a computationally feasible theoretical method for studying simultaneously the low-energy excitations and fundamental processes in atomic nuclei. Especially, we consider the results for a single β decay between even-mass nuclei quite encouraging, as they represent a crucial step toward the computation of the $\beta\beta$-decay nuclear matrix elements between even-even nuclei. Work along this direction is in progress and will be reported in near future.

ACKNOWLEDGMENTS

The work of K.N. is financed within the Tenure Track Pilot Programme of the Croatian Science Foundation and the École Polytechnique Fédérale de Lausanne, and the Project TTP-2018-07-3554 Exotic Nuclear Structure and Dynamics, with funds of the Croatian-Swiss Research Programme. The work of L.M.R. was supported by Spanish Ministry of Economy and Competitiveness (MINECO) Grant No. PGC2018-094583-B-I00.

[1] A. Faessler and F. Simkovic, J. Phys. G: Nucl. Part. Phys. **24**, 2139 (1998).
[2] J. Engel and J. Menéndez, Rep. Prog. Phys. **80**, 046301 (2017).
[3] P. Sarriguren, E. M. de Guerra, and A. Escuderos, Nucl. Phys. A **691**, 631 (2001).
[4] F. Šimkovic, V. Rodin, A. Faessler, and P. Vogel, Phys. Rev. C **87**, 045501 (2013).
[5] P. Pirinen and J. Suhonen, Phys. Rev. C **91**, 054309 (2015).
[6] T. Marketin, L. Huther, and G. Martínez-Pinedo, Phys. Rev. C **93**, 025805 (2016).
[7] M. T. Mustonen and J. Engel, Phys. Rev. C **93**, 014304 (2016).
[8] J.-U. Nabi and M. Böyükata, Nucl. Phys. A **947**, 182 (2016).
[9] T. R. Rodríguez and G. Martínez-Pinedo, Phys. Rev. Lett. **105**, 252503 (2010).
[10] J. M. Yao, L. S. Song, K. Hagino, P. Ring, and J. Meng, Phys. Rev. C **91**, 024316 (2015).
[11] K. Langanke and G. Martínez-Pinedo, Rev. Mod. Phys. **75**, 819 (2003).
[12] E. Caurier, G. Martínez-Pinedo, F. Nowacki, A. Poves, and A. P. Zuker, Rev. Mod. Phys. **77**, 427 (2005).
[13] M. Honma, T. Otsuka, T. Mizusaki, M. Hjorth-Jensen, and B. A. Brown, J. Phys.: Conf. Ser. **20**, 7 (2005).
[14] N. Shimizu, J. Menéndez, and K. Yako, Phys. Rev. Lett. **120**, 142502 (2018).
[15] S. Yoshida, Y. Utsuno, N. Shimizu, and T. Otsuka, Phys. Rev. C **97**, 054321 (2018).
[16] F. Dellagiacoma and F. Iachello, Phys. Lett. B **218**, 399 (1989).
[17] P. Navrátil and J. Dobes, Phys. Rev. C **37**, 2126 (1988).
[18] F. Iachello and P. Van Isacker, *The Interacting Boson-Fermion Model* (Cambridge University Press, Cambridge, 1991).
[19] N. Yoshida, L. Zuffi, and S. Brant, Phys. Rev. C **66**, 014306 (2002).
[20] L. Zuffi, S. Brant, and N. Yoshida, Phys. Rev. C **68**, 034308 (2003).
[21] S. Brant, N. Yoshida, and L. Zuffi, Phys. Rev. C **70**, 054301 (2004).
[22] S. Brant, N. Yoshida, and L. Zuffi, Phys. Rev. C **74**, 024303 (2006).
[23] J. Barea and F. Iachello, Phys. Rev. C **79**, 044301 (2009).
[24] N. Yoshida and F. Iachello, Prog. Theor. Exp. Phys. **2013**, 043D01 (2013).
[25] E. Mardones, J. Barea, C. E. Alonso, and J. M. Arias, Phys. Rev. C **93**, 034332 (2016).
[26] K. Nomura, N. Shimizu, and T. Otsuka, Phys. Rev. Lett. **101**, 142501 (2008).
[27] S. Brant, V. Paar, and D. Vretenar, Z. Phys. A: At. Nucl. **319**, 355 (1984).
[28] K. Nomura, R. Rodríguez-Guzmán, and L. M. Robledo, Phys. Rev. C **101**, 024311 (2020).
[29] F. Iachello and O. Scholten, Phys. Rev. Lett. **43**, 679 (1979).
[30] S. Goriely, S. Hilaire, M. Girod, and S. Péru, Phys. Rev. Lett. **102**, 242501 (2009).
[31] J. Decharge, M. Girod, and D. Gogny, Phys. Lett. B **55**, 361 (1975).
[32] L. M. Robledo, T. R. Rodríguez, and R. R. Rodríguez-Guzmán, J. Phys. G: Nucl. Part. Phys. **46**, 013001 (2019).
[33] K. Nomura, R. Rodríguez-Guzmán, and L. M. Robledo, Phys. Rev. C **96**, 014314 (2017).
[34] K. Nomura, R. Rodríguez-Guzmán, and L. M. Robledo, Phys. Rev. C **96**, 064316 (2017).
[35] K. Nomura, R. Rodríguez-Guzmán, and L. M. Robledo, Phys. Rev. C **99**, 034308 (2019).
[36] K. Nomura, R. Rodríguez-Guzmán, and L. M. Robledo, Phys. Rev. C **101**, 014306 (2020).
[37] T. Otsuka, A. Arima, and F. Iachello, Nucl. Phys. A **309**, 1 (1978).
[38] O. Scholten, Prog. Part. Nucl. Phys. **14**, 189 (1985).
[39] J. M. Arias, C. E. Alonso, and M. Lozano, Phys. Rev. C **33**, 1482 (1986).
[40] I. Morrison, A. Faessler, and C. Lima, Nucl. Phys. A **372**, 13 (1981).
[41] J. N. Ginocchio and M. W. Kirson, Nucl. Phys. A **350**, 31 (1980).
[42] K. Nomura, N. Shimizu, and T. Otsuka, Phys. Rev. C **81**, 044307 (2010).
[43] F. Dellagiacoma, Beta decay of odd mass nuclei in the interacting boson-fermion model, Ph.D. thesis, Yale University, 1988.
[44] J. Beringer, J. F. Arguin, R. M. Barnett, K. Copic, O. Dahl, D. E. Groom, C. J. Lin, J. Lys, H. Murayama, C. G. Wohl, W. M. Yao, P. A. Zyla, C. Amsler, M. Antonelli, D. M. Asner, H. Baer, H. R. Band, T. Basaglia, C. W. Bauer, J. J. Beatty, V. I. Belousov, E. Bergren, G. Bernardi, W. Bertl, S. Bethke, H. Bichsel, O. Biebel, E. Blucher, S. Blusk, G. Brooijmans, O. Buchmueller, R. N. Cahn, M. Carena, A. Ceccucci, D. Chakraborty, M. C. Chen, R. S. Chivukula, G. Cowan, G. D'Ambrosio, T. Damour, D. de Florian, A. de Gouvêa, T. DeGrand, P. de Jong, G. Dissertori, B. Dobrescu,

M. Doser, M. Drees, D. A. Edwards, S. Eidelman, J. Erler, V. V. Ezhela, W. Fetscher, B. D. Fields, B. Foster, T. K. Gaisser, L. Garren, H. J. Gerber, G. Gerbier, T. Gherghetta, S. Golwala, M. Goodman, C. Grab, A. V. Gritsan, J. F. Grivaz, M. Grünewald, A. Gurtu, T. Gutsche, H. E. Haber, K. Hagiwara, C. Hagmann, C. Hanhart, S. Hashimoto, K. G. Hayes, M. Heffner, B. Heltsley, J. J. Hernández-Rey, K. Hikasa, A. Höcker, J. Holder, A. Holtkamp, J. Huston, J. D. Jackson, K. F. Johnson, T. Junk, D. Karlen, D. Kirkby, S. R. Klein, E. Klempt, R. V. Kowalewski, F. Krauss, M. Kreps, B. Krusche, Y. V. Kuyanov, Y. Kwon, O. Lahav, J. Laiho, P. Langacker, A. Liddle, Z. Ligeti, T. M. Liss, L. Littenberg, K. S. Lugovsky, S. B. Lugovsky, T. Mannel, A. V. Manohar, W. J. Marciano, A. D. Martin, A. Masoni, J. Matthews, D. Milstead, R. Miquel, K. Mönig, F. Moortgat, K. Nakamura, M. Narain, P. Nason, S. Navas, M. Neubert, P. Nevski, Y. Nir, K. A. Olive, L. Pape, J. Parsons, C. Patrignani, J. A. Peacock, S. T. Petcov, A. Piepke, A. Pomarol, G. Punzi, A. Quadt, S. Raby, G. Raffelt, B. N. Ratcliff, P. Richardson, S. Roesler, S. Rolli, A. Romaniouk, L. J. Rosenberg, J. L. Rosner, C. T. Sachrajda, Y. Sakai, G. P. Salam, S. Sarkar, F. Sauli, O. Schneider, K. Scholberg, D. Scott, W. G. Seligman, M. H. Shaevitz, S. R. Sharpe, M. Silari, T. Sjöstrand, P. Skands, J. G. Smith, G. F. Smoot, S. Spanier, H. Spieler, A. Stahl, T. Stanev, S. L. Stone, T. Sumiyoshi, M. J. Syphers, F. Takahashi, M. Tanabashi, J. Terning, M. Titov, N. P. Tkachenko, N. A. Törnqvist, D. Tovey, G. Valencia, K. van Bibber, G. Venanzoni, M. G. Vincter, P. Vogel, A. Vogt, W. Walkowiak, C. W. Walter, D. R. Ward, T. Watari, G. Weiglein, E. J. Weinberg, L. R. Wiencke, L. Wolfenstein, J. Womersley, C. L. Woody, R. L. Workman, A. Yamamoto, G. P. Zeller, O. V. Zenin, J. Zhang, R. Y. Zhu, G. Harper, V. S. Lugovsky, and P. Schaffner (Particle Data Group), Phys. Rev. D **86**, 010001 (2012).

[45] Brookhaven National Nuclear Data Center, http://www.nndc.bnl.gov.